ELSEVIER

Catalysis Today 71 (2001) 21–29

CATALYSIS TODAY

www.elsevier.com/locate/cattod

Morphological effects of SnO_2 thin film on the selective oxidation of methane

Takashi Kawabe [a], Kenji Tabata [a,c,*], Eiji Suzuki [a,c], Yoko Ichikawa [a], Yosuke Nagasawa [b]

[a] *Research Institute of Innovative Technology for the Earth (RITE), 9-2 Kizugawadai, Kizu-cho, Soraku-gun, Kyoto 619-0292, Japan*
[b] *Osaka Gas Co., Ltd., Utilization Technology Department, Gas Appliance R&D Team, 1-1-3 Hokkou-Shiratsu, Konohana-ku, Osaka 554-0041, Japan*
[c] *Nara Institute of Science and Technology, Graduate School of Materials Science (NAIST), 8916-5 Takayama-cho, Ikoma, Nara 630-0101, Japan*

Abstract

The morphological effects of SnO_2 thin film on catalytic activities and selectivities for the selective oxidation of CH_4 were investigated with X-ray photoelectron spectroscopy (XPS) and thermal desorption spectroscopy (TDS). Dense texture type and a columnar texture type SnO_2 thin films were prepared by the sputtering method. The measured proportion of adsorbed oxygen species (O^{2-}, $O_2{}^{2-}$, $O_2{}^-$ and O_b) on these two types of samples with XPS were different from each other, and the proportion of a highly reactive oxygen species O^- was larger on the dense sample. The TDS data of the products (HCHO, CH_3OH, CO, CO_2 and H_2O) were obtained on the two different structured film samples after CH_4 exposure at room temperature. The obtained TPD data were explained appropriately by considering several reaction pathways. The dense texture type SnO_2 film showed a higher reactivity for the oxidation of CH_4 than that of the columnar texture type one. The selective formation of HCHO was especially observed for the dense texture film. The oxidation of CH_4 was therefore strongly affected by the surface morphology of SnO_2 film.

Keywords: Methane; Methanol; Formaldehyde; Tin oxide; Catalysts; Partial oxidation

1. Introduction

The selective oxidation reaction of hydrocarbon species on metal oxides has been practically and scientifically important process. The factors which affect the yield of the products in the reaction have been intensively studied. The structural sensitivity of the selective oxidation on crystallized metal oxides have been examined [1]. This means the determination of the structure of the active site and to what extend this structure can modify the reaction rate on the selectivity. Furthermore, these catalytic could be strongly affected by the presence of defective sites.

SnO_2 is widely used as a gas sensing device and the catalyst of oxidation reaction [2–6]. The reactive oxygen species of SnO_2 which play an important role in the oxidation was considered to be O^- species chemisorbed on the bridging oxygen site of the (1 1 0) surface [6]. Recently, we reported on the gas sensitivity control by the morphological variation of SnO_2 thin film [7]. In this paper, we reported that the gas sensitivity of a dense texture type SnO_2 film in contact with H_2 was much larger than that of a columnar texture type SnO_2 film. Furthermore, we studied CH_3OH

* Corresponding author. Tel.: +81-774-75-2305; fax: +81-774-75-2318.
E-mail address: kenjt@rite.or.jp (K. Tabata).

0920-5861/01/$ – see front matter
PII: S0920-5861(01)00444-8

adsorption on SnO_2 thin films with different morphologies [8]. In that paper, we reported that the dense texture type film oriented mainly to the (1 1 0) phase showed a higher reactivity for oxidation of CH_3OH than the columnar texture type film. Cox and co-workers [9] studied the CH_3OH dissociation and oxidation over the single crystal of SnO_2 (1 1 0) using X-ray photoelectron spectroscopy (XPS) and thermal desorption spectroscopy (TDS). In that paper, they reported that the formation of HCHO by the decomposition of adsorbed methoxide species occurred at two different types of oxygen vacancies on the (1 1 0) face. These results indicated that the catalytic properties over SnO_2 surface could be affected by the variation of morphology of that. However, the detail of the structural sensitivity of SnO_2 was still unclear. In this study, we examine the morphological effects in the selective oxidation of CH_4 with an SnO_2 thin film.

2. Experimental section

Two different types of SnO_2 thin films were prepared on a sapphire substrate by the reactive radiofrequency (RF) magnetron sputtering method (SPF-430: Nichiden Anelva). We called these two different SnO_2 films as a dense texture type film and a columnar texture type one. The details of the sputtering conditions are written in [7]. Three-dimensional images of the surface of SnO_2 films were obtained using the scanning electron microscope (SEM) with S-5000 (Hitachi). The acceleration voltage of electron was 10.0 kV. The X-ray diffraction spectrum of these films were shown in our previous paper [8]. XPS measurements were performed with an angle-resolved ESCA-KM (Shimadzu). An Al Kα X-ray source was used for the excitation, and the pass energy was 32 eV. The central position of the sample was measured with XPS. The diameter of the elliptically measured region was 2 mm × 1 mm. XPS was detected at an angle of 15° to the surface of the sample. The binding energy (E_B) was calibrated with respect to the peak position of the Sn^{4+} ($3d_{5/2}$) peak as 486.8 eV [8]. The treatments of acquired spectra were carried out with the software (VISION: Kratos Analytical). O_2 gas (>99.8% purity, Sumitomo Seika Chemicals) was used through a liquid nitrogen trap. Highly purified CH_4 gas (>99.9995% purity, Teisan) was used. TDS measurements were carried out with a quadrapole mass spectrometer QMS-200 (Balzers Instruments) attached to the vacuum chamber of XPS (base pressure $= 4 \times 10^{-7}$ Pa). The treatments of acquired mass spectra were carried out with the software (QuadStar 422: Balzers Instruments). The raising rate of temperature was 5 K/min. Sample heating was carried out with a halogen lamp, which was attached at the outside of the second chamber of XPS. The estimated measurement error was within ±2 K. Heat treatments during the XPS measurements were carried out with a resistive heater, which was built in a sample holder in an analyzing chamber. The estimated measurement error was within ±10 K. The specific surface area of SnO_2 thin film was measured with the BET method (BELSORP TCV: Nippon-bel).

3. Results

3.1. SEM images of SnO_2 film

Fig. 1 shows the SEM images of dense (a) and columnar (b) texture type films. The appearance of these images was clearly different. The smooth surface of the dense sample can be seen but several nanometer size of the column can be seen in the SEM image of the columnar sample. From the results of our previous XRD measurements of these films, it was found that the dense texture film had a strong peak of the (1 1 0) phase and the columnar one had main peaks of the (2 1 1) and (3 0 1) phases [8]. The specific surface area of these films was measured by BET method (Table 1). The measured area of the columnar type film was almost 20 times larger than that of the dense texture type film.

3.2. XPS measurements of SnO_2 thin films

3.2.1. Oxidized SnO_2 films

In the beginning, we checked the surface components of these samples in advance with XPS. All the observed peaks were originated from Sn, O and the contaminating carbon. In order to obtain the information of adsorbed oxygen species on the surface, we carried out XPS measurements on the pre-oxidized SnO_2 films. Fig. 2 shows the O (1s) level spectra of two different types of films, obtained after O_2

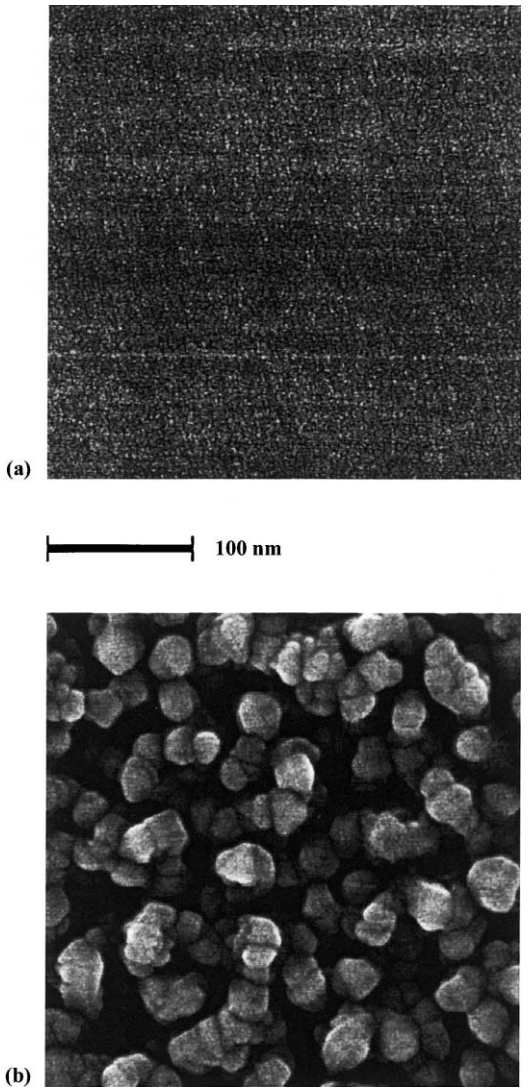

Fig. 1. SEM images of SnO_2 thin films for: (a) dense texture type film; (b) columnar texture type film.

oxidization at 473 K at 1.36×10^{10} L. We resolved the spectra into several peaks as to match with the original ones with the software. Every peak position of the resolved spectra was the same in Fig. 2(a) and (b). The peak positions and their proportions were listed in Table 2. The resolved peak at $E_B = 530.6$ eV could be assigned to the lattice oxygen atoms (O^{2-}). Concerning the resolved peaks at $E_B = 532.4$ eV, we assigned to O_2^{2-} species from the reported peak

Table 1
Specific BET areas of SnO_2 films (the corrected BET area)

Dense (cm^2/substrate area)	6.15
Columnar (cm^2/substrate area)	121

position of O_2^{2-} on nickel and copper [10,11]. The resolved peak at $E_B = 531.5$ eV could be assigned to O^- species from the reported peak position of O^- on nickel [12–14]. Concerning the resolved peak at $E_B = 529.3$ eV, we assumed to be oxygen species ionically chemisorbed on the bridging sites (O_b) from the results of our previous report [15]. The small resolved peak at $E_B = 533.9$ eV was observed in Fig. 2(b). We assumed that this peak was able to be assigned to O_2^- species because the peak position of superoxo was reported to be at ca. 534.5 eV on Li–O_2 complexes [16]. The proportions of resolved peaks were different between two samples. The total value of the proportions of O^- and O_b on the columnar type film was clearly smaller than that on the dense type film as shown in Table 2. In the previous paper, we reported that an adsorbed oxygen atom coupled with the nearest neighboring bridging oxygen vacant site was O^- species and this oxygen species brought catalytic activity on the (1 1 0) surface of SnO_2 [17]. Furthermore, we suggested O_b species shifted to O^- during the oxidation of CH_4 [17]. Therefore, the difference of the proportions of the reactive oxygen species were originated from the different morphologies.

3.2.2. *CH_4-exposed SnO_2 films*

In order to investigate the difference of reactivities on these two different structured samples, we carried out CH_4 exposure on the pre-oxidized samples. Fig. 3 shows the C (1s) level spectra obtained after CH_4 exposure at room temperature and at 1.36×10^6 L. We resolved each spectrum into five peaks using the software. Every peak position of resolved spectra was the same between these two different samples. The peak positions of resolved peaks and their intensity proportion were listed in Table 3. The resolved hydrocarbon species at $E_B = 284$–285 eV could be assigned to the methyl group formed from adsorbed CH_4 and further carbonized species [18,19]. The resolved peak at $E_B = 286.4$ eV could be assigned to methoxide species since the peak position of methoxide species adsorbed on both ZnO and TiO_2 were reported to

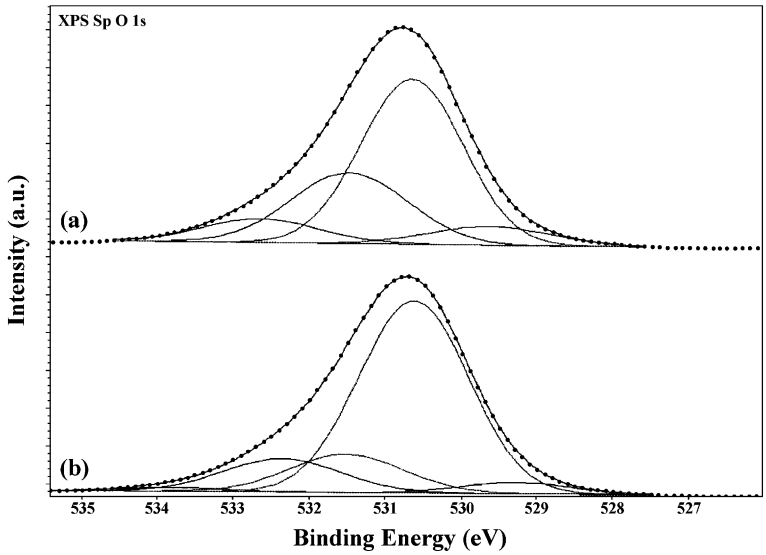

Fig. 2. O (1s) level XPS spectra of SnO_2 thin films obtained after O_2 exposure: (a) dense texture type film; (b) columnar texture type film. O_2 exposure was carried out at 473 K at 1.36×10^{10} L.

be $E_B = 286.8$ eV [20,21]. The resolved peak at ca. $E_B = 287.4$ eV could be assigned to molecularly adsorbed CH_3OH from the reported E_B of molecularly adsorbed one on ZnO (287.3 eV) and TiO_2 (0 0 1) (287.4 eV) [20,21]. Concerning the assignment of the last resolved peak at $E_B = 288.9$ eV, two hydrocarbon species, i.e. formate or dioxymethylene species could be considerable from the reported value (~289.3 eV) adsorbed on ZnO or ZrO_2 [20,22]. Dioxymethylene species was also observed after CH_3OH adsorption on SnO_2 with FTIR in our previous study [23]. We therefore assigned the peak to the dioxymethylene species. On the columnar texture type SnO_2 film, both methoxide species and molecularly adsorbed CH_3OH proportions were larger than those on the dense texture type film (Table 3). On the contrary, the intensity proportion of dioxymethylene species on the dense texture type film was more than three times larger than that on the columnar texture film. Since the proportion of this highly oxidized species on the dense sample was larger than that on the columnar one, the reactivity for the oxidation of CH_4 on the dense texture film was supposed to be higher than that on the columnar sample.

Table 2
Intensity proportion of surface oxygen species of SnO_2 films obtained after O_2 exposure (O_2 exposure was carried out at 473 K and at 1.36×10^{10} L)

	Species				
	O^{2-}	O_2^{2-}	O_2^-	O^-	O_b
E_B (eV)	530.6	532.4	533.9	531.5	529.3
Dense	56	9	–	27	8
Columnar	68	13	1	14	4

3.3. Thermal desorption spectroscopy

3.3.1. O_2 desorption from oxidized SnO_2 films

In order to investigate the thermal stability of chemisorbed oxygen species on the surface, thermal desorption of oxygen molecule was carried out on the pre-oxidized SnO_2 films. Fig. 4 shows the TDS data of the dense texture type SnO_2 film (a) and the columnar one (b). O_2 exposure was carried out under the same condition as that of XPS measurements. Heating rate was 5 K/min, and $m/z = 32$ was detected. TDS data of the dense sample started to rise from around 573 K, and that of the columnar sample rose from around 530 K. The spectrum (a) had a peak at around 700 K, and spectrum (b) had a peak at around 600 K. The TDS of O_2 from the single crystal of SnO_2 (1 1 0)

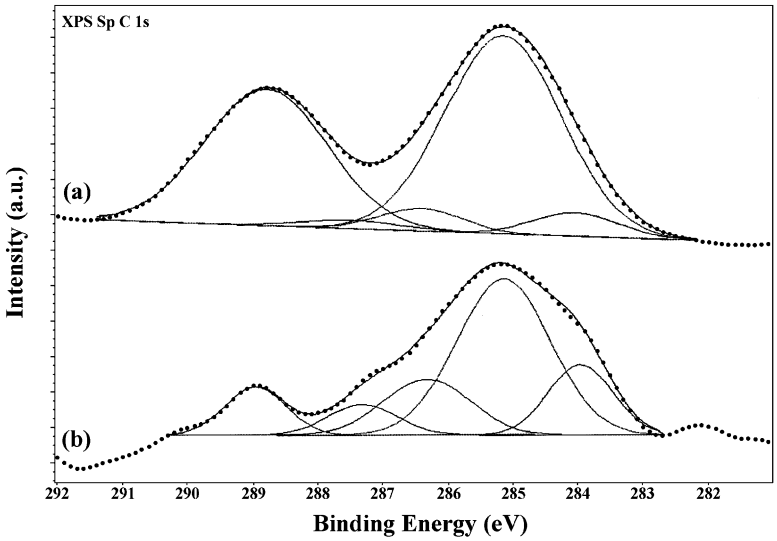

Fig. 3. C (1s) level XPS spectra of oxidized SnO_2 thin films obtained after following CH_4 exposure. (a) is of dense texture type film, and (b) is of columnar texture type film, respectively. CH_4 exposure was carried out at room temperature at 1.36×10^{10} L.

Table 3
Intensity proportion of surface intermediate species of oxidized SnO_2 films obtained after CH_4 exposure (CH_4 exposure was carried out at room temperature and at 1.36×10^6 L)

	Species			
	Methyl group	CH_3O^-	CH_3OH	H_2COO^{2-}
E_B (eV)	285.1/284	286.4	287.4	288.9
Dense	57	6	2	35
Columnar	63	15	9	13

surface was investigated by Cox and co-workers [9]. They reported that bridging oxygen desorption was observed over a wide range of examined temperature region (300–600 K). Recently, we studied the thermal desorption of adsorbed oxygen from the dense texture type SnO_2 film using XPS [24]. In that study, we reported that three surface oxygen species (O^-, O_2^{2-}, O_2^-) were observed on the surface after O_2 exposure, and that these oxygen species were desorbed in the order of O^-, O_2^{2-} (>473 K) and O_2^- (>673 K). These results corresponded to the order of theoretically calculated value of stabilization energy using a point-charge model on the reduced SnO_2 (1 1 0) surface [25]. The desorption temperature of O_2 was, therefore, considered to be strongly affected by its electronic states and surface structure. The different desorption spectra in Fig. 4(a) and (b) should represent the presence of different adsorbed oxygen states on those two different structured SnO_2 thin films.

3.3.2. Oxidized species desorption from SnO_2 films after CH_4 exposure

3.3.2.1. SnO_2 dense texture type film. In the previous section, we mentioned the difference of surface

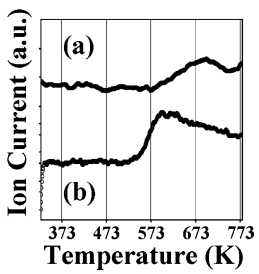

Fig. 4. TDS data of O_2 with dense (a), and columnar (b) texture type SnO_2 films obtained after O_2 exposure. O_2 exposure was carried out at 473 K and at 1.36×10^{10} L. The detected $m/z = 32$ (O_2).

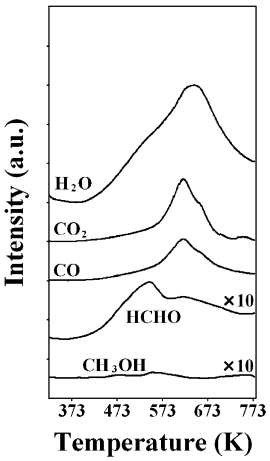

Fig. 5. TDS data of the oxidized products with SnO_2 dense texture type film. O_2 exposure was carried out at 473 K and at 1.36×10^{10} L. CH_4 exposure was carried out at room temperature and at 1.36×10^{10} L.

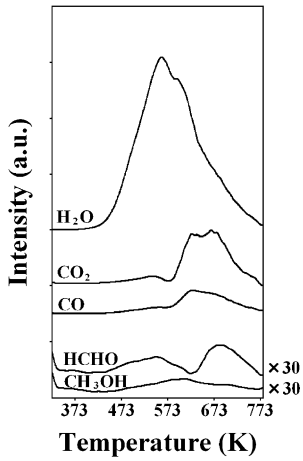

Fig. 6. TDS data of the oxidized products with SnO_2 columnar texture type film. O_2 exposure was carried out at 473 K and at 1.36×10^{10} L. CH_4 exposure was carried out at room temperature and at 1.36×10^{10} L.

oxygen species between two types of SnO_2 films, which should lead the difference of reactivities in the oxidation of CH_4. In order to investigate the reactivity of oxygen species and selectivity in the oxidized products, we carried out CH_4 exposure on the SnO_2 thin films. Pre-oxidation was carried out at 1.36×10^{10} L and at 473 K. After evacuation, CH_4 exposure was carried out at 1.36×10^{6} L and at room temperature. The TDS data of the dense sample are shown in Fig. 5. The observed TDS data of each component after only O_2 exposure was subtracted from each TDS data as the background. The main desorbed products were H_2O, CO_2 and CO. CO and CO_2 mainly desorbed at around 620 K and their shoulder peaks were observed at a higher temperature around 670 K. These variations of CO and CO_2 spectra were almost the same. H_2O desorbed over a wide range of temperature variations. The main peak was at around 640 K, and the shoulder peak was observed at around 530 K. Small amount of HCHO was desorbed at around 530 K and it had a broad peak at around 620 K. The first peak position of HCHO was in good agreement with the shoulder peak of H_2O spectrum. The peak position of main peak of H_2O spectrum was in good agreement with those peak position of CO and CO_2. A slight desorbed CH_3OH was also observed, however, its variation was obscure.

3.3.2.2. SnO_2 columnar texture type film. The similar TDS data of SnO_2 columnar texture type film were observed as shown in Fig. 6. Both CO and CO_2 were desorbed from around 600 K and had the peak at around 620 K. Another peak of CO_2 spectrum was observed at around 670 K and the broad peak of CO spectrum covered around this temperature. These variations of the columnar sample were different from those in Fig. 5. The main and shoulder peaks of desorbed H_2O spectrum were observed at ca. 530 and 590 K. These values were smaller than that of the dense sample. HCHO and CH_3OH were also observed. The thermal desorption spectrum of HCHO had two peaks at around 530 and 670 K. The slight desorption peak of CH_3OH was observed at around 620 K. The peak position of the second peak of HCHO spectrum was in accordance with that of the second peak of CO_2. The peak position of CH_3OH desorption was agreed with those of CO and CO_2 desorption. The observed TDS data with those different structured samples represented the morphological effects.

3.3.3. Evaluation of reactivity and selectivity after CH_4 exposure

The total amount of accumulated intensity of each desorbed component in Figs. 5 and 6 were calculated up to 773 K, then normalized with each measured

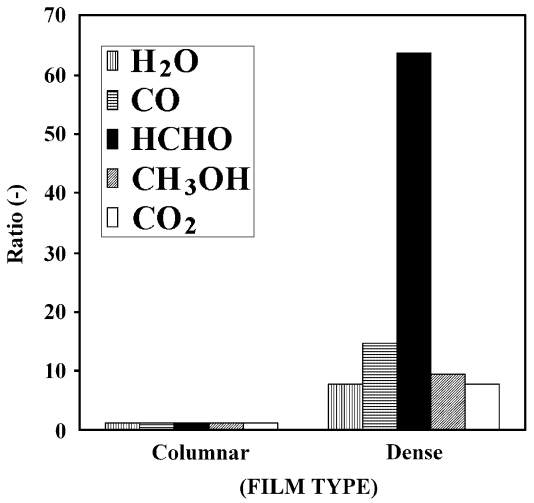

Fig. 7. Calculated ratios of the desorbed products. The amount of each oxidized products desorbed from columnar texture type film was assumed to be 1.

surface area. The normalized intensity of each component of the dense sample was divided by that of the same component of the columnar sample. The calculated ratio of each component was shown in Fig. 7. The total value of each component of the dense sample was clearly larger than that of the columnar sample. Furthermore, the normalized ratio of desorbed HCHO from the dense sample was clearly larger than other desorbed components. This means the selective formation of HCHO over the dense texture type SnO_2 thin film.

4. Discussion

CH_4 oxidation on the surface of SnO_2 has been considered to be initiated by the extraction of H atom by the active O^- species:

$$CH_4 + O^- \rightarrow CH_3^\bullet + OH^- \quad (1)$$

$CH_3^\bullet$ could be subsequently oxidized to $CH_2^\bullet$ and $CH^\bullet$. Some part of $CH_3^\bullet$ could be reacted to methoxide:

$$CH_3^\bullet + O^- \rightarrow CH_3O^- \quad (2)$$

Recently, we studied the oxidation reaction route of adsorbed CH_3OH on SnO_2 powder using FTIR [23]. In that paper, we reported that dioxymethylene species was produced from the hydroxylation of methoxide on SnO_2 at 373 K:

$$CH_3O^- + OH^- \rightarrow CH_2OO^{2-} + H_2 \quad (3)$$

Dioxymethylene species observed in the C (1s) XPS spectra (Fig. 3) was assumed to be produced via this reaction route after CH_4 exposure at room temperature. Produced dioxymethylene species is considered to be desorbed as HCHO:

$$CH_2OO^{2-} \rightarrow HCHO + O^{2-} \quad (4)$$

Since the decomposition of dioxymethylene species to HCHO was considered to occur easily with the rise of temperature from the results of our recent study [26], HCHO desorption observed in TDS data for both types of SnO_2 films (Figs. 5 and 6) at a lower temperature region (ca. 530 K) could be derived from the decomposition of dioxymethylene species. Concerning the formation of H_2O, the combination of OH^- species produced by the reaction route in Eq. (1) was considered:

$$2OH^- \rightarrow H_2O + O^{2-} \quad (5)$$

HCHO could also be formed through the oxidation of methoxide species:

$$CH_3O^- + O^- \rightarrow HCHO^- + OH^- \quad (6)$$

$$HCHO^- \rightarrow HCHO + e^- \quad (7)$$

The desorbed HCHO at around 620 K observed in Fig. 5 could be formed by these reaction routes. The oxidation of $HCHO^-$ (Eq. (6)) should be accompanied as follows:

$$CH_2O^- + O^- \rightarrow CHO^- + OH^- \quad (8)$$

$$CHO^- + O^- \rightarrow CO^- + OH^- \quad (9)$$

$$CO^- + O^- \rightarrow CO_2{}^{2-} \quad (10)$$

The simultaneous desorption of CO and CO_2 at around 620 K observed in Fig. 5 was assumed to be explicable using these oxidation mechanisms. SnO_2 dense texture film oriented mainly to (1 1 0) surface was considered to have a higher reactivity for the oxidation of CH_4 because the presence of a larger amount of the active O^- species on the surface.

On the SnO_2 columnar texture type film, the selective formation of CH_3OH was observed at around 620 K as shown in Fig. 6. Concerning the formation of CH_3OH, some kinds of reaction routes were suggested:

$$CH_3O^- + OH^- \rightarrow CH_3OH + O^{2-} \quad (11)$$

$$CH_3O^- + H_2O \rightarrow CH_3OH + OH^- \quad (12)$$

$$CH_3^\bullet + OH^- \rightarrow CH_3OH^- \quad (13)$$

CH_3OH formation by the reaction routes in Eqs. (11) and (12) should be accompanied by the formation of dioxymethylene species and the following formation of formaldehyde. Dioxymethylene species and formaldehyde were assumed to be formed by the reaction routes in Eqs. (3), (4) and (6), (7). Since the lowering of HCHO spectrum at ca. 620 K observed in Fig. 6 suggested that the desorbed CH_3OH could be formed by the reaction route in Eq. (13). The first step of CH_4 oxidation reaction on SnO_2 (1 1 0) has been considered to produce OH^- species and methyl radicals as shown in Eq. (1). Produced methyl radicals were considered to combine with the neighboring O^- species promptly and, therefore, methoxide species were generated as shown in Eq. (2). On the surface of dense texture type film, this reaction routes were assumed to be more favorable on account of the larger amount of O^- species. Produced methoxide and OH^- species were considered to form dioxymethylene species easily by the reaction routes in Eq. (3), which caused a larger amount of dioxymethylene species in the surface as shown in Table 3. The proportion of O^- species on the surface of the columnar texture type film was smaller than that on the dense texture type film. On the surface of columnar texture type film, we speculated that the formation route of CH_3OH in Eq. (13) could be more favorable than the route in Eq. (2) on account of a smaller amount of O^- species. Molecularly adsorbed CH_3OH formed by the reaction route in Eq. (13) was assumed to be easily dehydrogenated by the neighboring OH^- species:

$$CH_3OH + OH^- \rightarrow CH_2OH + H_2O \quad (14)$$

$$CH_2OH + OH^- \rightarrow HCHO + H_2O \quad (15)$$

$$HCHO + OH^- \rightarrow CHO + H_2O \quad (16)$$

$$CHO + OH^- \rightarrow CO + H_2O \quad (17)$$

$$CO + OH^- \rightarrow CO_2 + H \quad (18)$$

The simultaneous desorption of CO and CO_2 together with the desorption of CH_3OH observed in Fig. 6 could be explicable by these reaction routes. Thus, the selective formation of intermediate species, i.e. CH_3OH, HCHO was assumed to be strongly affected by the morphology of SnO_2 film. The desorption peak of HCHO, CO and CO_2 appeared again at around 670 K in Fig. 6. We speculated that this formation of HCHO was originated from the oxidation of methoxide species with a less reactive oxygen species. We found that this columnar texture type film had strong peaks of (2 1 1) and (3 0 1) phases from our previous XRD measurements [8]. We assumed that the reaction between the oxygen species on these faces and methoxide species was occurred at a higher temperature region. Therefore, the larger desorption peaks of the components (HCHO, CO and CO_2) at around 670 K observed for the columnar texture film (Fig. 6) indicated the contribution from a larger amount of a less reactive oxygen species on the surface of the SnO_2 columnar texture film.

5. Conclusion

The dense texture type SnO_2 film showed a higher reactivity for the oxidation of CH_4 than that of the columnar texture type one. The selective formation of HCHO was especially observed for the dense texture film. The oxidation of CH_4 was therefore strongly affected by the surface morphology of SnO_2 film.

Acknowledgements

This study was financially supported by the NEDO.

References

[1] J.H. Tatibouët, Appl. Catal. A 148 (1997) 213.
[2] J.M. Themlin, R. Sporken, J. Darville, R. Caudanno, J.M. Gilles, Phys. Rev. B 42 (1990) 11914.
[3] G. Gaggiotti, A. Galdikas, S. Kačiulis, G. Mattongo, A. Šetkus, J. Appl. Phys. 76 (1994) 4467.
[4] G.L. Shen, R. Casanova, G. Thornton, Vacuum 43 (1992) 1129.

[5] P.A. Cox, P.G. Egdell, W.R. Flavell, R. Helbig, Vacuum 33 (1983) 835.
[6] P.M.A. Sherwood, Phys. Rev. B 41 (1990) 10151.
[7] Y. Nagasawa, K. Tabata, H. Ohnishi, Appl. Surf. Sci. 121–122 (1997) 327.
[8] T. Kawabe, K. Tabata, E. Suzuki, Y. Nagasawa, Surf. Sci. 482–485 (2001) 183.
[9] V.A. Gercher, D.F. Cox, J.M. Themlin, Surf. Sci. 306 (1994) 279.
[10] J.P.S. Badyal, X. Zhang, R.M. Lambert, Surf. Sci. Lett. 225 (1990) L15.
[11] P.V. Kamath, C.N.R. Rao, J. Phys. Chem. 88 (1984) 464.
[12] M.S. Hedge, M. Ayyoob, Surf. Sci. 173 (1986) L635.
[13] C.N.R. Rao, V. Vijayakrishnam, G.U. Kulkarni, M.K. Rajumon, Appl. Surf. Sci. 84 (1995) 285.
[14] G.U. Kulkarni, C.N.R. Rao, M.W. Roberts, Langmuir 11 (1995) 2572.
[15] T. Kawabe, K. Tabata, E. Suzuki, Y. Yamaguchi, Y. Nagasawa, J. Phys. Chem. 105 (2001) 4239.
[16] S.L. Qiu, C.L. Lin, J. Chen, M. Strongin, Phys. Rev. B 39 (1989) 6194.
[17] Y. Yamaguchi, Y. Nagasawa, S. Shimomura, K. Tabata, E. Suzuki, Chem. Phys. Lett. 316 (2000) 477.
[18] T. Kawabe, S. Shimomura, T. Karasuda, K. Tabata, E. Suzuki, Y. Yamaguchi, Surf. Sci. 448 (2000) 101.
[19] J.G. Serafin, C.M. Friend, J. Phys. Chem. 93 (1989) 1998.
[20] J.M. Vohs, M.A. Barteau, Surf. Sci. 91 (1986) 176.
[21] K.S. Kim, M.A. Barteau, Surf. Sci. 13 (1989) 223.
[22] J.M. Vohs, M.A. Barteau, Surf. Sci. 109 (1988) 197.
[23] F. Ouyang, S. Yao, K. Tabata, E. Suzuki, Appl. Surf. Sci. 158 (2000) 28.
[24] Y. Nagasawa, T. Choso, T. Karasuda, S. Shimomura, F. Ouyang, K. Tabata, Y. Yamaguchi, Surf. Sci. 433–435 (1999) 226.
[25] Y. Yamaguchi, Y. Nagasawa, A. Murakami, K. Tabata, Int. J. Quant. Chem. 69 (1998) 669.
[26] T. Kawabe, K. Tabata, E. Suzuki, Y. Yamaguchi, Y. Nagasawa, Surf. Interf. Anal. 29 (2000) 791.